A PROPOSED TACTICAL ANTISUBMARINE WARFARE DEVICE UTILIZING RESONANT BUBBLES

Sherman E. Wright

NAVAL POSTGRADUATE SCHOOL
Monterey, California

THESIS

A PROPOSED TACTICAL ANTISUBMARINE
WARFARE DEVICE UTILIZING
RESONANT BUBBLES

by

Sherman E. Wright, Jr.

December 1973

Approved for public release; distribution unlimited.

A Proposed Tactical Antisubmarine Warfare Device Utilizing Resonant Bubbles

by

Sherman E. Wright, Jr.
Lieutenant, United States Navy
B.S., United States Naval Academy, 1968

Submitted in partial fulfillment of the
requirements for the degree of

MASTER OF SCIENCE IN ENGINEERING ACOUSTICS

from the

NAVAL POSTGRADUATE SCHOOL
December 1973

ABSTRACT

An experimental investigation was made of the scattering properties of a bubble cloud in a sound field in a fresh water medium. The size of the bubbles was on the order of 0.125 cm radius, and was far above resonant size for the ensonifying sound field. It was determined that the bubbles scattered coherently in the forescatter direction, and incoherently in the backscatter direction. Based upon the scattering properties of the bubble cloud, it appears feasible to develop a device that could have tactical applications in the prosecution of long-range submarine contacts held by active sonars. Such a device would utilize the principle of resonant bubbles, and would require approximately 2.5 cubic feet of air (corrected to STP) to maintain a +20dB target strength for five minutes of continuous operation.

TABLE OF CONTENTS

LIST OF TABLES

LIST OF DRAWINGS

I. INTRODUCTION

This paper is concerned with developing a deployable device that will assist aircraft in prosecuting submarine targets detected by active sonars.

There are areas of uncertainty associated with sonar detections. At long ranges this uncertainty area can be considerable since the uncertainty area increases as the range to the target increases. In essence, bearing and range data from the sonar consoles serve only to locate the center of the uncertainty area. For long-range targets a second search must be conducted within the uncertainty area if fire control data are required.

There are three major factors that contribute to the formation of uncertainty areas. The first is the presence of inhomogenities in the ocean that affect the sound velocity profile and create an "acoustic" uncertainty as to the target's exact position. Secondly, sonar equipment limitations expand the uncertainty area. The third source of uncertainty is due to errors introduced while trying to position the aircraft directly over the target's position as determined by the sonar. Normally the aircraft would be given a vector (bearing and range) from the ship to the target. Equipment calibration error (sonar, radar, gyroscope, compass, etc.) or human error can easily cause the aircraft to position itself incorrectly.

The requirement to further localize the target presents two major problems. Additional resources must be expended to locate the target, but more importantly, the searching aircraft are susceptible to detection by the submarine. It takes time to conduct a search, and aircraft have limited sonobuoy payloads and station-time constraints that may require additional units to complete the attack. At long ranges target classification is particularly difficult; therefore, it is essential that the target is not alerted by the searching aircraft. Evasive maneuvers by the target at long ranges from the ship will usually result in the loss of contact by the sonar.

II. THEORY

A. CONCEPT

If the attacking unit were to deploy a device that was visible to both the sonar holding contact on the target and to the aircraft pilot, the localization phase could be eliminated. With the sonar holding contact on both the target and the device, a second vector (attack vector) could be given from the sonar console data using the device as a reference point.

The prosecuting unit would proceed to the target uncertainty area by using the sonar data as an initial positioning vector. Once the unit was in position, the device would be deployed. When the sonar detects the device an attack vector can be given, using the device as a reference point. The attacking aircraft would then fly directly over the device at a low altitude and follow the attack vector to the weapon launch point.

This method of attack has two main advantages: (1) It can be rapidly executed, and (2) the units are less susceptible to detection. Although there are uncertainty areas associated with both the target and the device, the attack vector is based upon the bearing and range resolution (discrimination) of the sonar and not on the true geographical positions.

B. THE DEVICE

The envisioned device would utilize resonant-size bubbles to gain a target strength comparable to that of a submarine (a +20 dB target strength is assumed). Hopefully this device would be economically more attractive than a transponder buoy, and the reflections would be less suspicious because of their "mushy" nature (as observed experimentally). The envisioned device and assembly are illustrated in Figure 1.

The launching and operation of the device should be as noiseless as possible. A drag parachute could be attached to reduce water entry noise, and the device could be operated at a low air pressure to help limit bubble generation noise. The bubbles would be generated by forcing air through the holes in the manifold. The result would be a sheet of bubbles with each bubble undergoing hydrostatic expansion as it rises to the surface. In research, it was observed that bubble size was a function of the hole diameter, the thickness (length) of the hole, the forcing air pressure, and the depth of water above the bubble device. By controlling these factors, bubbles could be generated with specific dimensions to be at resonance with the excitation frequency of the sonar when they reached a depth of 50 feet.

The size of the device is largely determined by the air requirements. The air requirements depend upon the length of time the +20 dB target strength must be maintained. The device must operate long enough to allow for the sonar to detect it, but if the operating period is too long, it may

complicate the situation. The attacking unit may have to deploy more than one device before detection by the sonar could be gained and, due to the movement of the target or the sonar, the previously undetected devices may appear as false targets. As a consequence, all calculations in this section are based upon five minutes of continuous operation, with the bubbles resonant at a depth of 50 feet.

C. CALCULATIONS

1. Reference 1 gives the following expression for the target strength of a single bubble:

$$TS = 10 \log \frac{a^2}{(f_r^2/f^2 - 1)^2 + \delta^2} \quad , \tag{1}$$

where a = bubble radius;

δ = damping constant;

f_r = resonant frequency;

f = excitation frequency.

The resonant frequency is given [Ref. 1] by

$$f_r = \frac{1}{2\pi a} \sqrt{\frac{3\gamma P_o}{\rho}} \quad , \tag{2}$$

where a = bubble radius;

P_o = hydrostatic pressure;

γ = ratio of specific heat;

ρ = density of the water.

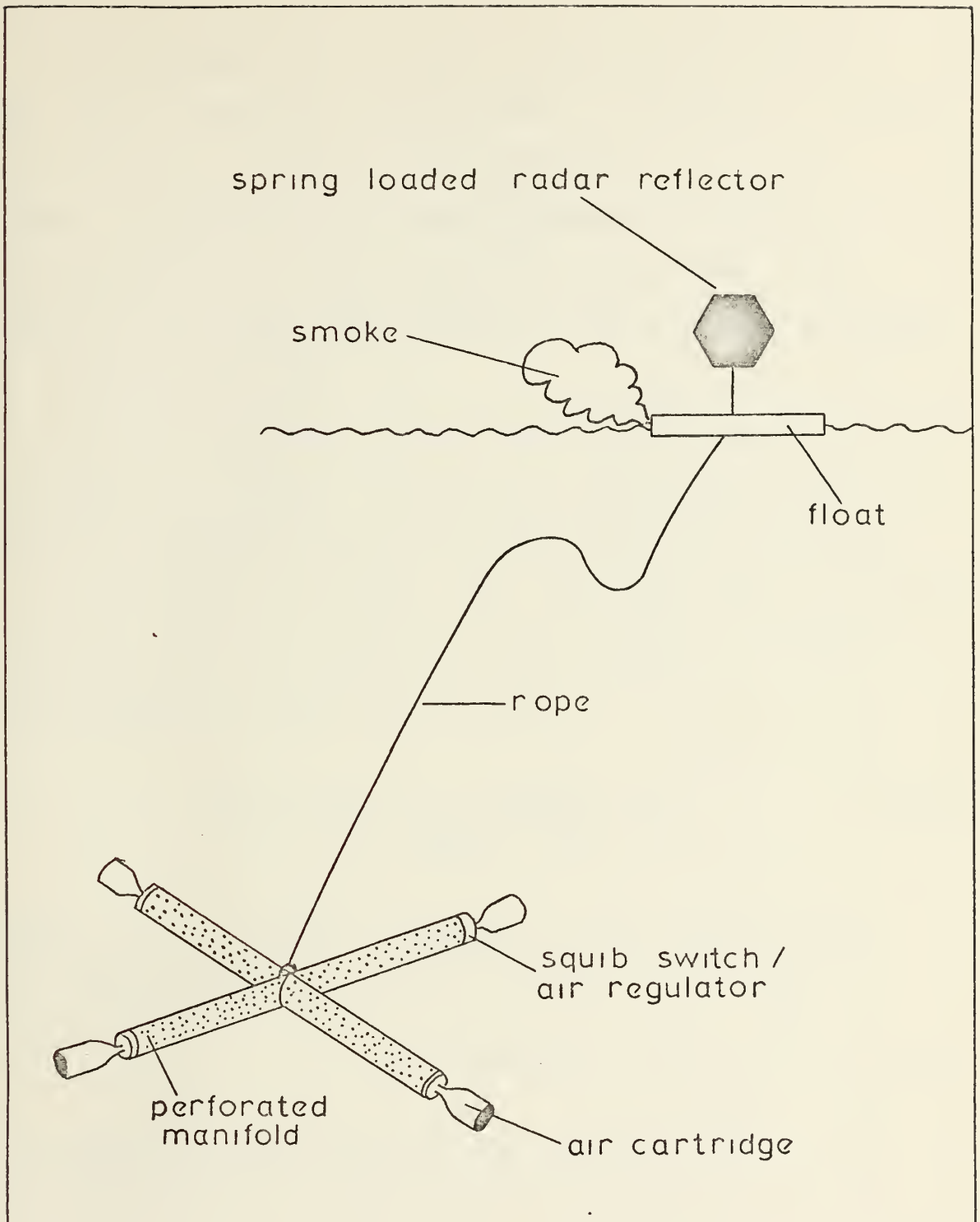

FIGURE 1: THE DEVICE

Calculations will be based on the frequency 3250 Hz. The target strength of a bubble that is resonant at a depth of 50 feet in sea water at this frequency is -27.3dB. Figure 2 illustrates the target strength of a bubble in a 3250 Hz field as it rises toward the sea surface. The bubble in the figure was assumed to have a 0.1586 cm radius at a depth of 50 feet.

If only the bubbles within three dB of a resonant target strength are included, and multiple scattering between the bubbles is neglected, the air requirements for the device can be estimated as follows: The required number of bubbles needed to initially produce a target strength of +20dB is found from an extension of Equation 1:

$$TS = 10 \log \frac{na^2}{(f_r^2/f^2 - 1)^2 + \delta^2} \qquad (3)$$

where n = number of bubbles in the acoustic beam.

The volume of air required at a 50-foot depth (V_{50}) is

$$V_{50} = \frac{4}{3} \pi n a^3 \qquad (4)$$

and correcting the volume to zero depth (V_0) is

$$\frac{V_{50}}{V_0} = (1 + \frac{D}{10})^{-1/3} \qquad (5)$$

where D is in meters.

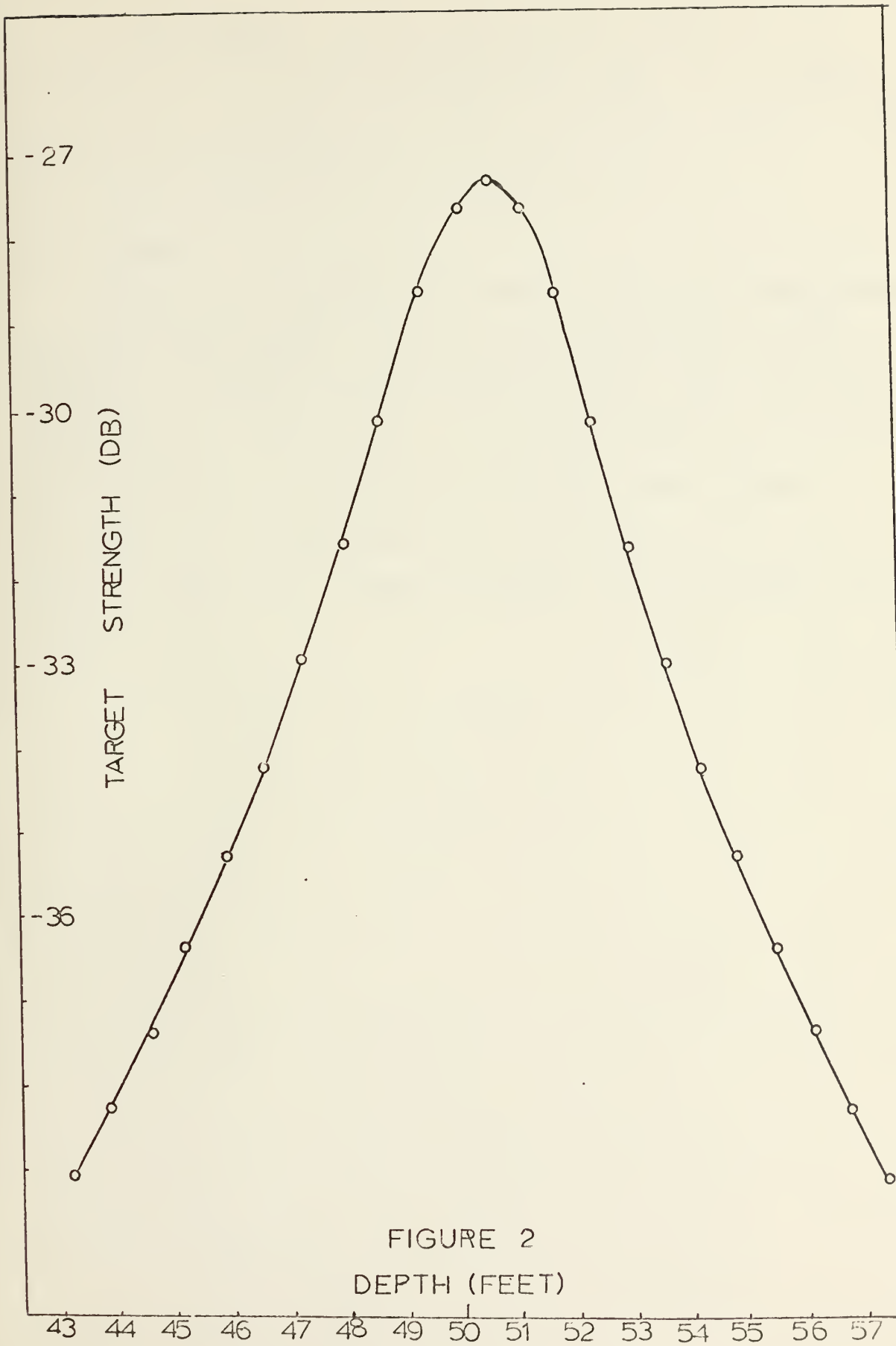
-27
-30
-33
-36
TARGET STRENGTH (DB)
43 44 45 46 47 48 49 50 51 52 53 54 55 56 57
DEPTH (FEET)

FIGURE 2

If the terminal velocity of a bubble in sea water is assumed to be 25 cm/sec [Ref. 2], the total air requirement (corrected to standard pressure) to maintain a target strength of +20dB for five minutes is 2.77 cubic feet.

D. SUMMARY

The critical assumption in Equation 3, used in determining the air requirements, was that the bubbles scattered incoherently. Another important assumption was that the bubbles would scatter isotropically. The final significant assumption was the neglect of multiple scattering between bubbles. It is these three assumptions that are investigated in this paper to determine if the approximate air requirements are valid.

III. EXPERIMENTAL PROCEDURE

A. THE BUBBLE GENERATOR

Early attempts in the laboratory failed to produce resonant sized bubbles for the frequency range of interest. Consequently, experiments were conducted with bubbles that were greater than the resonant size. Mechanical methods were chosen over electrolysis to produce the bubbles for two reasons. First, it was felt that mechanical means would provide better control of bubble size and bubble production rate; second, the method was the same as envisioned for the device. Five holes were drilled in a 60-cm piece of 1/2-inch diameter copper tubing. The holes were 0.0114 cm in diameter and were spaced 10.5 cm apart along the length of the tubing. A portable compressed air cylinder was used as the air supply unit. Air pressure was regulated to the bubble generator by means of needle valves and a pressure gage. The bubble generator was operated at a depth of 2.21 meters in fresh water at a constant air pressure of 7.5 psig. The tank was six feet wide and 24 feet long.

The holes in the copper tubing were numbered consecutively from one to five, with hole number one closest to the air inlet. The average bubble radius was found to be 0.125 cm (corrected to zero depth), with each hole producing the same sized bubble, but different bubble rates (bubbles per second). Individual holes were taped closed when not in use.

Bubble size was determined by capturing individual bubbles near the surface of the tank by means of an inverted glass beaker, then measuring the bubble diameter with a micrometer. By measuring the amount of time required for a bubble column to fill a volume of known size, the volume flow rates were determined. With the volume flow rates and bubble sizes known, the bubble rate (bubbles per second) could then be deduced. Table I indicates the observed bubble flow rates.

TABLE I: Bubble Flow Rates

Hole Number Open	Bubble Rate	Volume Flow Rate
1	153 bubbles/sec	1.25 ml/sec
1 and 2	296 bubbles/sec	2.42 ml/sec
1, 2, and 3	426 bubbles/sec	3.49 ml/sec
1, 2, 3, and 4	568 bubbles/sec	4.64 ml/sec
1, 2, 3, 4, and 5	678 bubbles/sec	5.54 ml/sec

B. FORESCATTER INVESTIGATION

A series of experiments was conducted to determine the acoustic signal scattered by the bubbles in the forescatter and backscatter directions. The basic circuit used in the investigation of forescatter is illustrated in Figure 3. The sine wave from the signal generator was amplified 20dB and was used to drive the F-27 transducer at five volts.

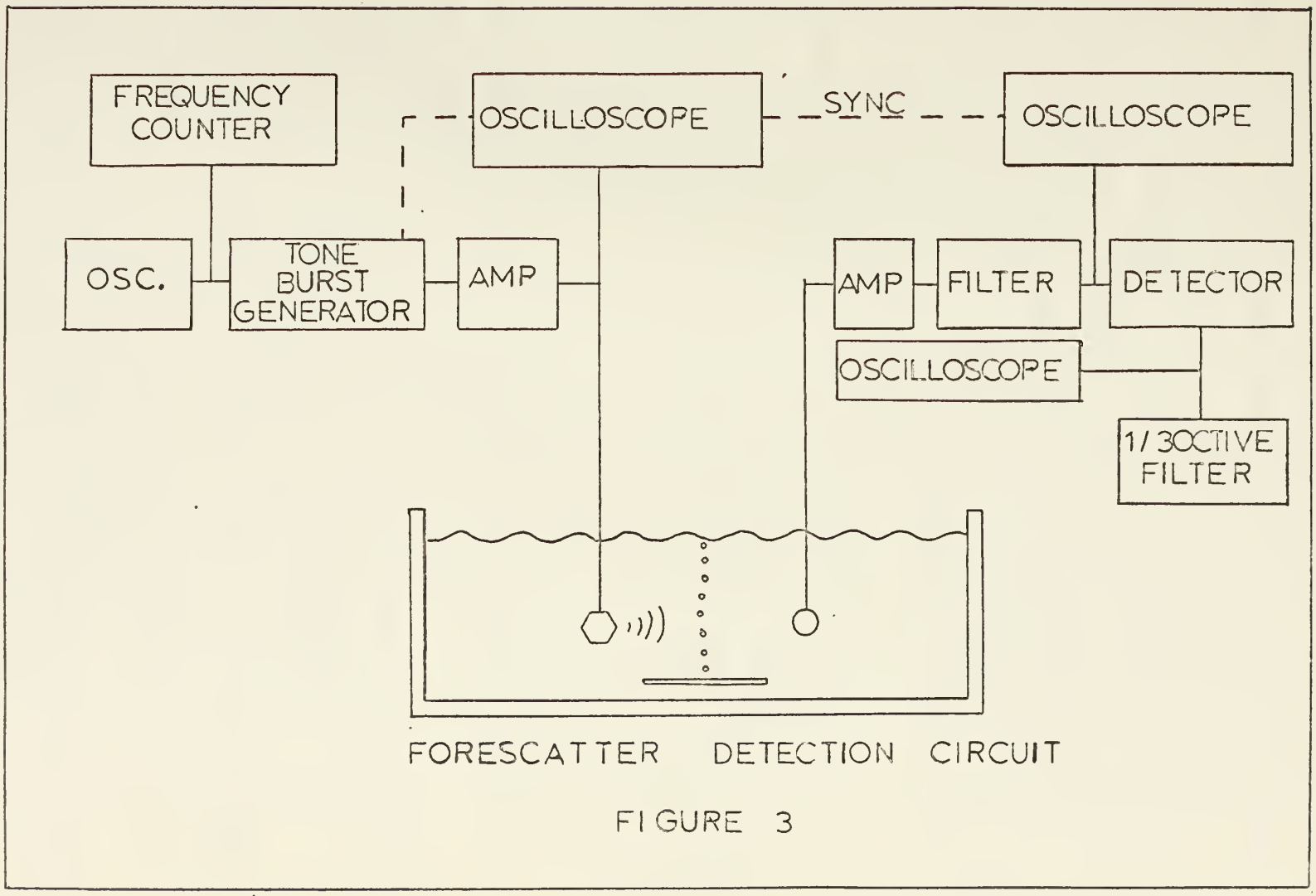
FREQUENCY COUNTER
OSCILLOSCOPE
SYNC
OSCILLOSCOPE
OSC.
TONE BURST GENERATOR
AMP
AMP
FILTER
DETECTOR
OSCILLOSCOPE
1/3OCTIVE FILTER
FORESCATTER DETECTION CIRCUIT

FIGURE 3

The bubble columns were positioned to coincide with the transducer-hydrophone axis in the far field region of the F-27. Typical separation distances were 120 cm between the transducer and the bubble column, and 100 cm from the bubble column to the hydrophone. After passing through the bubble cloud, the acoustic signal was received by the LC-32 hydrophone. The received signal was amplified 60dB, passed through a high-pass RC filter to remove the 60 Hz component, and then either viewed directly on an oscilloscope or passed through the envelope detector and analyzed.

Because the bubbles were large (0.125 cm radius), the acoustic signal was far above the resonant frequency of the bubbles (2.6 KHz). As the bubbles ascended toward the surface and passed through the sound field, the associated scattering of the sound by the bubbles caused amplitude modulation of the received signal. The envelope detector rectified and low passed the signal so fluctuation and spectral analysis could be conducted on the modulation signal.

A typical run would consist of generating a particular bubble rate, then changing the excitation frequency from 80 KHz to 25 KHz in 5 KHz steps. The run would then be repeated with no bubbles present in order to normalize the data. Comparison of the two runs then allows one to determine the scattering effect of the bubbles.

Typical sound pressure levels received by the LC-32 were in the range of 62 to 73db re 1 μbar. The signal-to-noise ratio was extremely frequency dependent, ranging from 45dB

at the high frequencies to 15dB at the low frequencies. The primary cause for this degradation of the signal-to-noise ratio was due to the poor impedance match between the amplifier and the transducer at low frequencies.

C. BACKSCATTER INVESTIGATION

The circuit used for the backscatter investigation required several modifications of the original forescatter circuit. The geometry and the circuit are illustrated by Figure 4.

It was observed that the F-27 transducer had significant side lobes perpendicular to the axis of propagation. This required the direct path signal to be baffled to prevent the backscatter signal from being completely masked by the direct path signal.

The sound pressure level of the backscatter signal at the hydrophone was in the 36 to 29dB range (re: 1 μbar), which required the preamps to be increased to 80dB. In order to combat the growing noise problem, an active Krohn-Hite filter was added to the circuit. The active filter was used as a band pass filter with a bandwidth of 10 KHz, centered on the excitation frequency.

Due to the fluctuating nature of the backscatter signal, the signal-to-noise ratio varied greatly with time and also as a function of frequency. Typical peak values of the signal were 15dB above the noise at the high frequencies, and 10dB or less at the low frequencies. Figures 5 and 6 illustrate

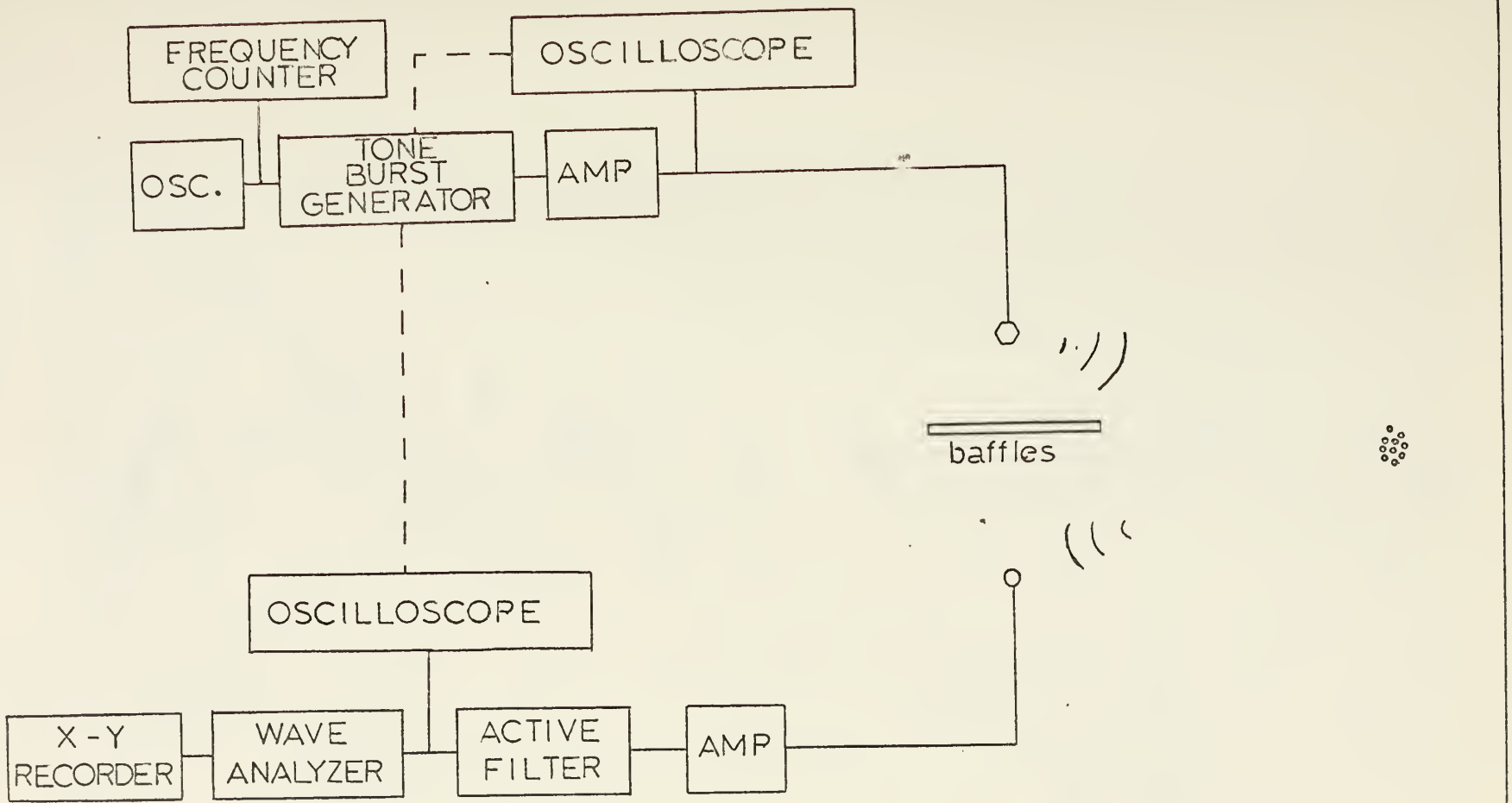

BACKSCATTER DETECTION CIRCUIT

FIGURE 4

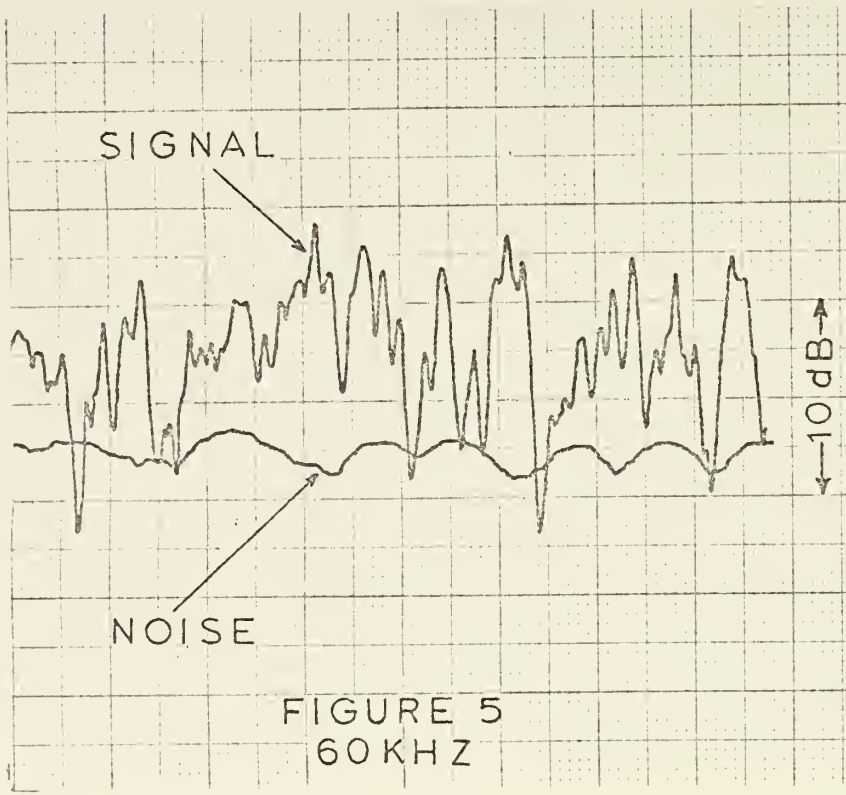

FIGURE 5
60 KHZ

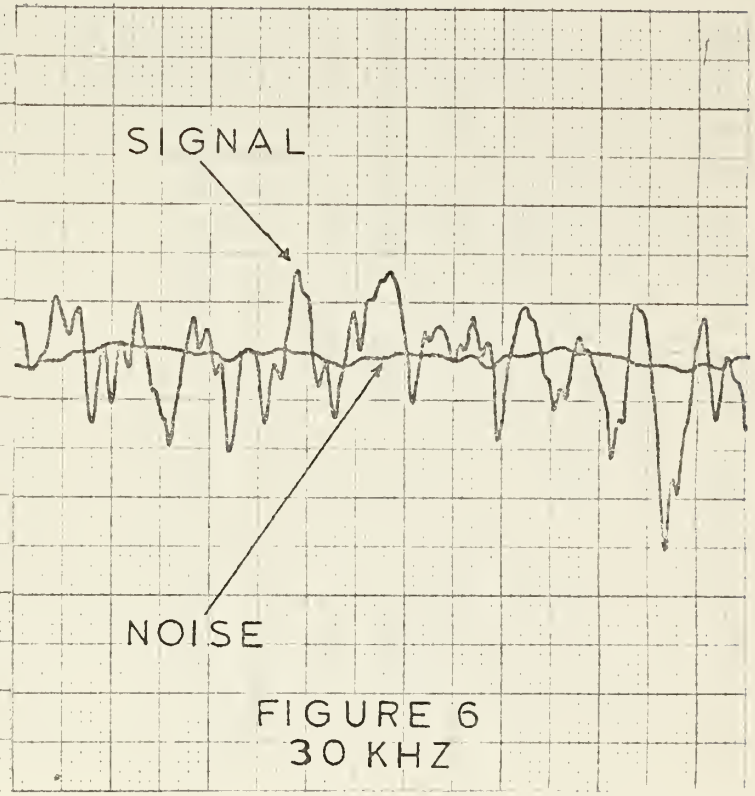

FIGURE 6
30 KHZ

the nature of the signal-to-noise levels at a high (60 KHz) and low (30 KHz) frequency. The signal portion of the figures was obtained by plotting on the X-Y recorder the continuous backscatter from a small bubble cloud. At 60 KHz the transducer ensonified 47 bubbles within the 3dB width of the major lobe, and at 30 KHz the transducer ensonified 93 bubbles. The noise portions of the figures were obtained on the X-Y recorder by plotting the received signal when no bubbles were present (no backscatter portion in the signal). A majority of the noise present was tank reverberation at the driving frequency.

IV. EXPERIMENTAL RESULTS

The experimental measurements of the acoustic scattering were used to calculate a value for the target strength of the bubble cloud in the forescatter and backscatter directions. From the target strength data, scattering on a per bubble basis could then be computed and analyzed.

A. FORESCATTER

1. Target Strength

From Ref. 1, one has the following definition for target strength:

$$TS \equiv 10 \log \left. \frac{I_r}{I_i} \right|_{r = 1} \qquad (6)$$

where I_r = intensity of return at one meter;

I_i = incident intensity.

Target strength calculations were based upon the geometrical arrangement of the experiment and the following calculations. In the following description it is convenient to refer to voltage rather than acoustic pressures. In all cases the voltage is proportional to the pressure, with the same constant of proportionality.

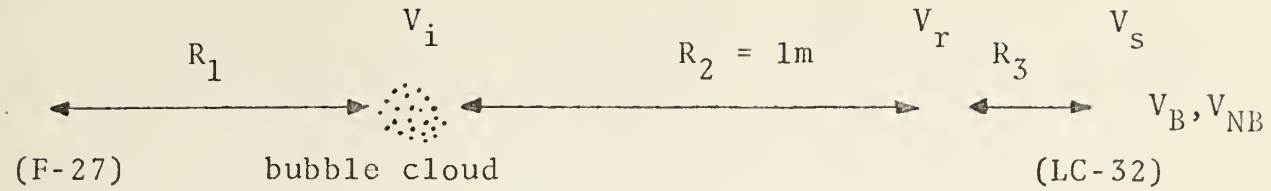

where V_i = voltage incident at geometric center of bubble cloud;

V_B = voltage received at LC-32 with bubbles present;

V_{NB} = voltage received at LC-32 with no bubbles present;

V_s = voltage scattered by bubbles received at hydrophone location;

V_r = voltage scattered by bubbles corrected to one meter.

Because the bubbles are driven above resonance, the acoustic pressure scattered in the forward direction is directly out of phase with the incident signal. Therefore, the reduction of the signal by the bubble cloud is a measure of the forescatter. Thus, one has the relationship $V_s = V_{NB} - V_B$, and therefore $V_r = \frac{R_2 + R_3}{R_2} V_s$ and $V_i = \frac{R_1 + R_2 + R_3}{R_1} V_{NB}$. In obtaining these equations it has been assumed that the incident field varies as $1/r$ measured from the F-27, and V_s varies as $1/r$ measured from the bubble cloud.

From Equation 6 it follows that $TS = 20 \log \frac{V_r}{V_i}$, which results in the relationship

$$TS = 20 \log \left[\frac{R_1(R_2 + R_3)}{R_2(R_1 + R_2 + R_3)} \left(1 - \frac{V_B}{V_{NB}}\right)\right] \qquad (7)$$

Figure 7 is a graph of target strength versus frequency for three different bubble flow rates. Runs 1 and 2 contained suspicious drops in target strength, and were probably due to experimental error.

Two possible methods were considered to determine the manner in which the bubbles contributed to the overall target strength. If all the bubbles radiated coherently in phase with one another, then the total radiated pressure would be proportional to the total number n of bubbles, and the target strength would be increased by 20 log n. However, if the bubbles radiated incoherently, the total radiated pressure would be proportional to the square root of the number of bubbles n, and the target strength would be increased by 10 log n.

The data used in Figure 7 were sampled at 35, 45, and 60 KHz to obtain average values for the change in target strength due to a change in the bubble flow rate. For Run 2, the bubble rate was increased by a factor of 1.9 over the flow rate during Run 1, and this resulted in an average gain of 6.5dB. In Run 3, the bubble rate was increased by a factor of 1.4 over the flow rate during Run 2, and the resultant gain was 3.9dB. Coherent scattering would predict a gain of 5.6dB in Run 2, and 2.9dB in Run 3, whereas incoherent scattering would predict a gain of 2.8dB in Run 2, and 1.5dB in Run 3. Table II summarizes these results, expressing the increase in the bubble flow rate as the ratio n. From Table II it is apparent that in the

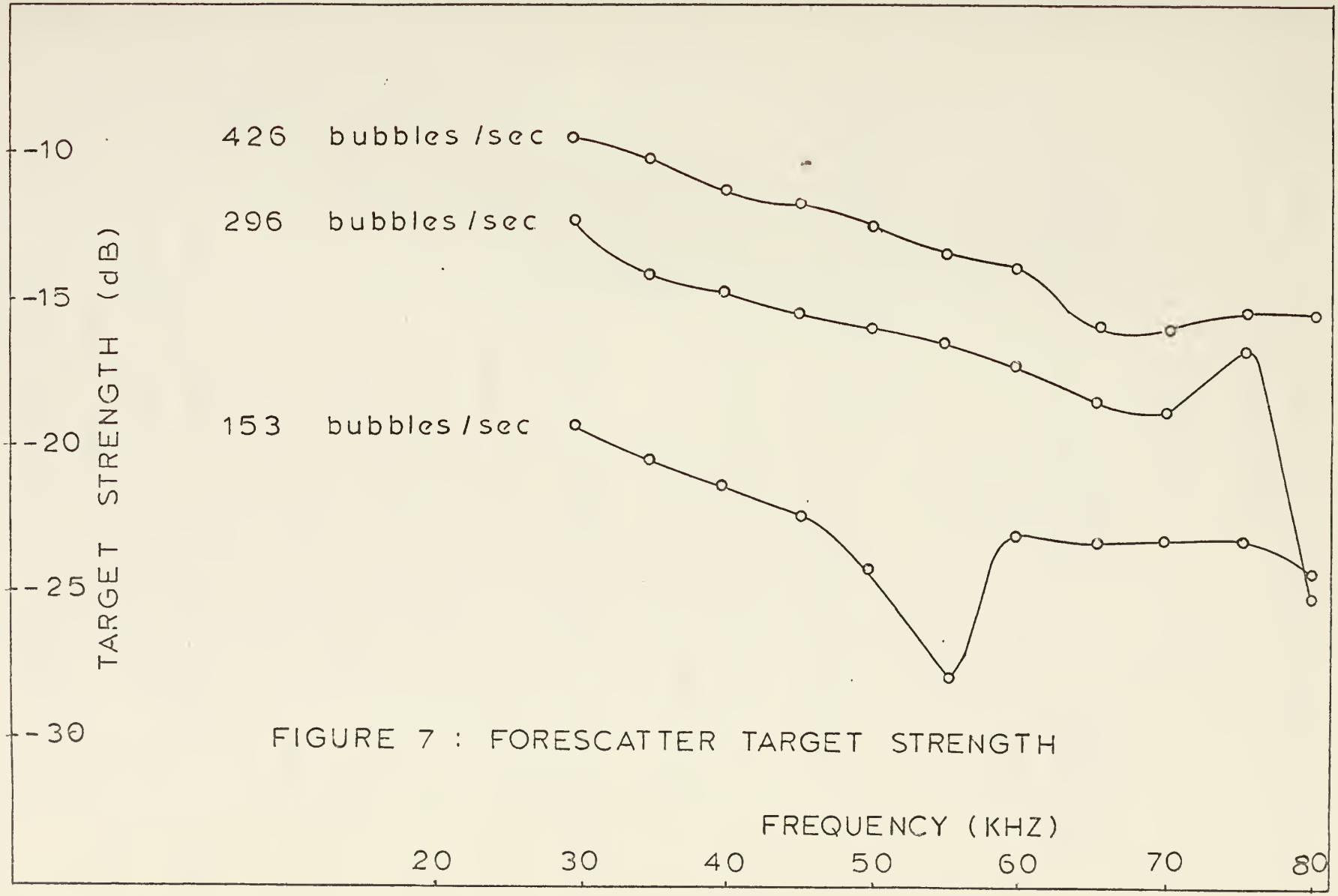

FIGURE 7 : FORESCATTER TARGET STRENGTH

forescatter mode of operation, the scattered signals tend to add together in a coherent manner.

TABLE II

n	Average Increase	Coherent Prediction	Incoherent Prediction
1.9	6.5dB	5.6dB	2.8dB
1.4	3.9dB	2.9dB	1.5dB

2. Fractional Scattering

Fractional scattering, as defined by Equation 8

$$TS \equiv 20 \log [\text{fractional scattering}] \qquad (8)$$

provides a better basis for calculations and comparisons than would logarithms.

Table III and Figure 8 compare theoretical fractional scattering to experimental values on a fractional scattering per bubble basis. The theoretical values were obtained from Equations 1, 2 and 8. The experimental values were obtained by dividing the fractional scattering values determined from target strength data and Equation 8 by the number of bubbles within the 3dB beam. In such a calculation it is implicitly assumed that the total scattered pressure is directly proportional to the number of bubbles. The close agreement between theory and experimental results in Table II bears out this assumption. Three runs were made with different bubble rates and the fractional scattering appeared to depend on the

TABLE III

Run	(bubbles/sec) Bubble Flow Rate	Fractional Scattering/Bubble	Standard Deviation	(per bubble) Target Strength
1	153	1.17×10^{-3}	0.138	-58.64dB
2	296	1.20×10^{-3}	0.125	-58.42dB
3	426	1.24×10^{-3}	0.059	-58.13dB
	theoretical	1.37×10^{-3}	0.004	-57.30dB

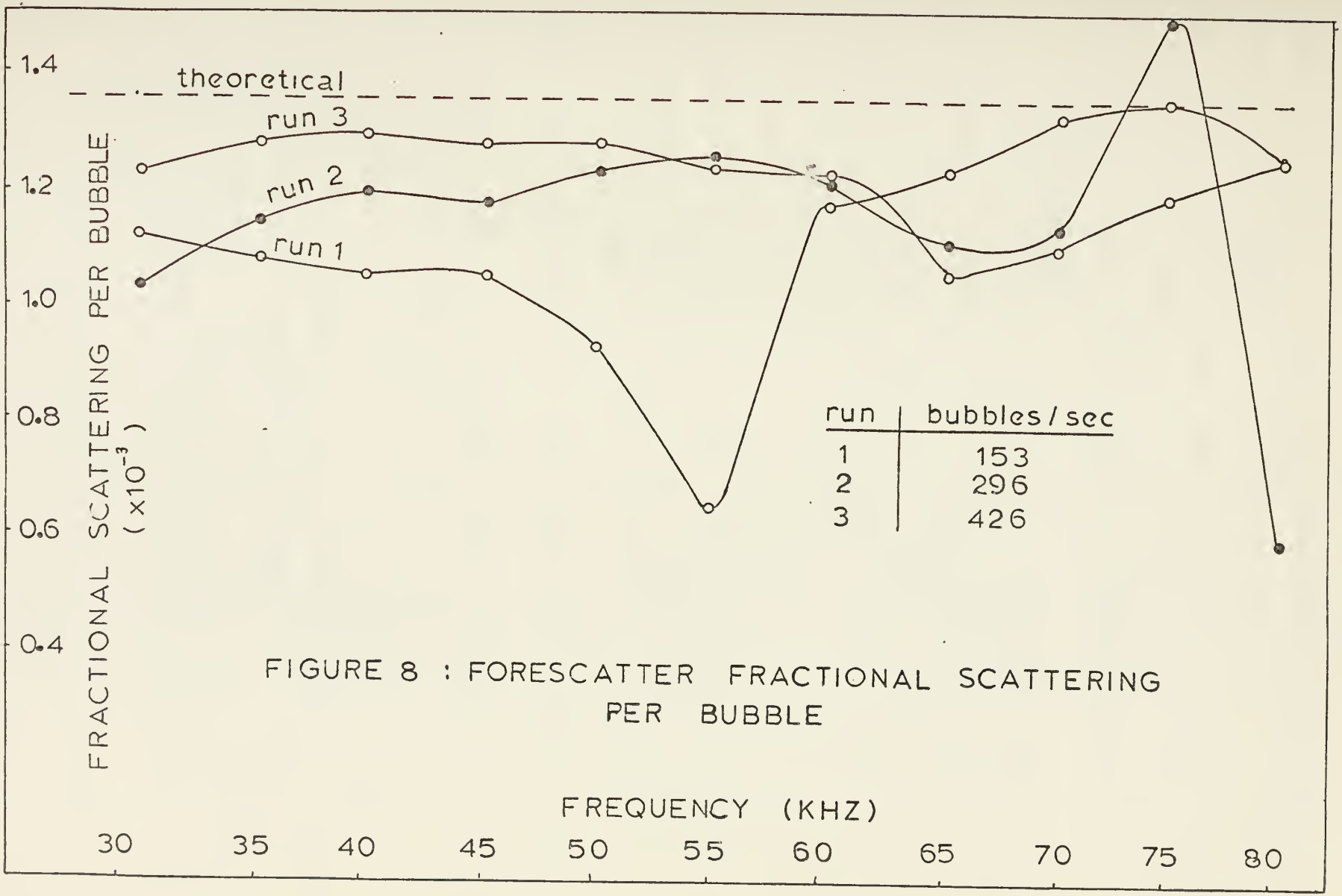

FIGURE 8 : FORESCATTER FRACTIONAL SCATTERING PER BUBBLE

bubble flow rate. The data were averaged and the standard deviation was computed. Table III indicates that at higher bubble flow rates the fractional scattering is greater and is closer to the theoretical value. Additionally, there is less deviation from the average at the higher bubble rates.

3. Fluctuations

The forescatter signal V_B (as defined on page 24) can be considered to have ac and dc components, where the ac portion of the signal fluctuates an amount V_{ac} about the dc component V_{dc}. The dc component was estimated visually on the oscilloscope as the average value of the received pulses. Deviations from this average were considered to be the ac component of the received signal. The per cent fluctuation is defined as the ac portion of the signal divided by the dc component, expressing this quotient as a percentage: $\frac{V_{ac}}{V_{dc}} \times 100$. Five runs were made, each with a different bubble flow rate. Figure 9 illustrates the fluctuations as a function of frequency for the different runs. Although the data tended to fluctuate within each run, the per cent fluctuations decreased with an increase in the excitation frequency. Overall values of per cent fluctuations increased as the bubble flow rate was increased. Table IV gives the per cent fluctuations obtained by averaging the fluctuation values from 35 to 80 KHz for each run.

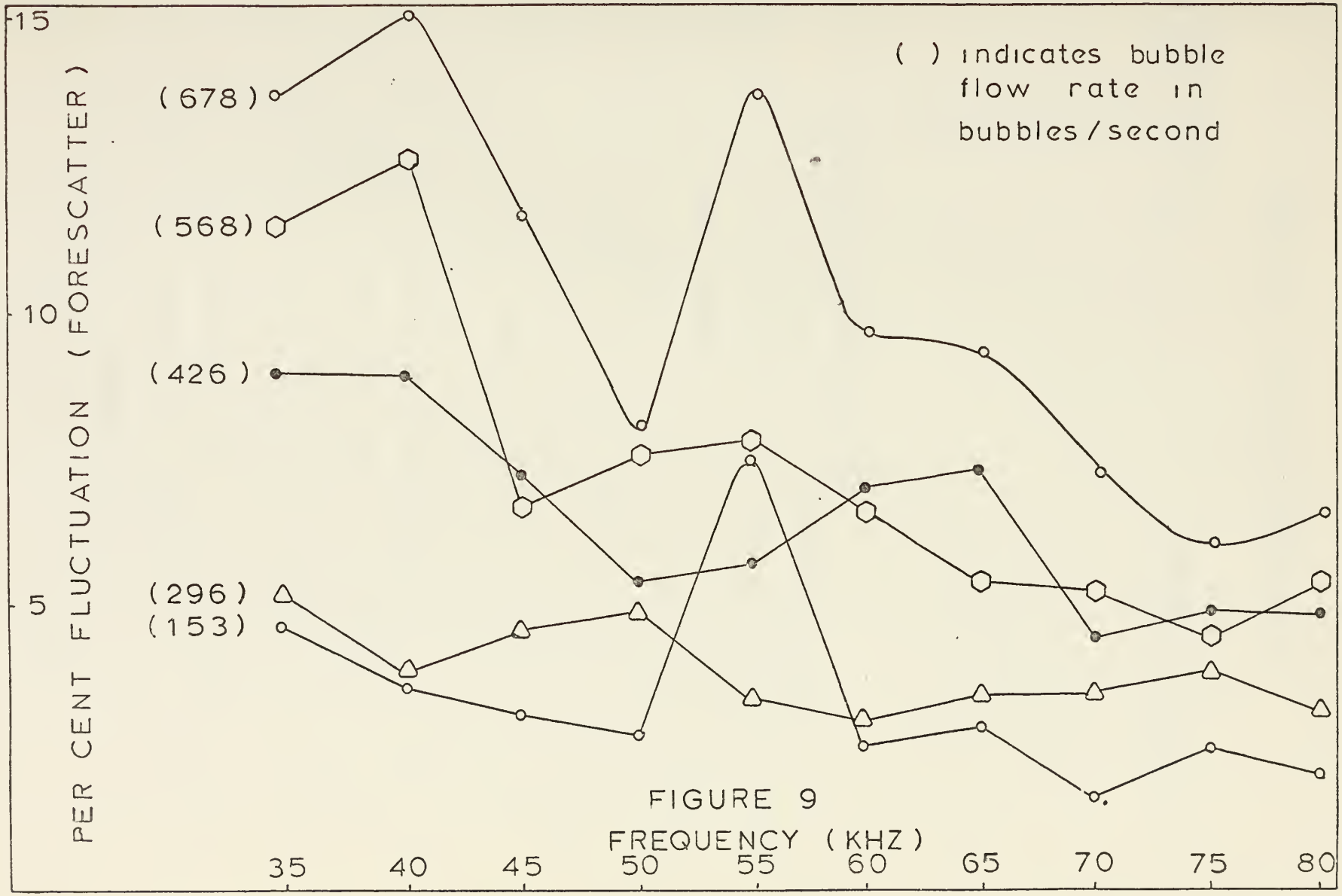
15
10
5
PER CENT FLUCTUATION (FORESCATTER)
( ) indicates bubble flow rate in bubbles/second
(678)
(568)
(426)
(296)
(153)
35
40
45
50
55
60
65
70
75
80
FREQUENCY (KHZ)

FIGURE 9

TABLE IV: Average % Fluctuations

(bubbles/sec) Bubble Flow Rate	Average % Fluctuations
153	3
296	4
426	6
568	7
678	9

4. Fluctuation Spectrum Level

The fluctuations of the forescatter signal were analyzed by passing the received signal through an envelope detector and then through the 1/3-octave filter, during continuous-wave transmission at 80 KHz. Five runs were made with varying bubble flow rates, and two of the frequency spectra are illustrated in Figure 10. All the results were similar, so only the highest and lowest bubble flow rates were plotted. A 10 log Δf correction factor was applied to the data; then the results were normalized to all pass. All of the runs were within four per cent of having 1/3 of the total energy in the envelope contained within the frequency band from 2.5 to 100 Hz. The peaks in the graphs at 63 Hz are due to 60-Hz electrical noise. The fluctuation spectra levels had slopes ranging from -12dB/decade to -33dB/decade in different frequency regions, indicating a higher energy content in the received signal envelope at the low frequencies.

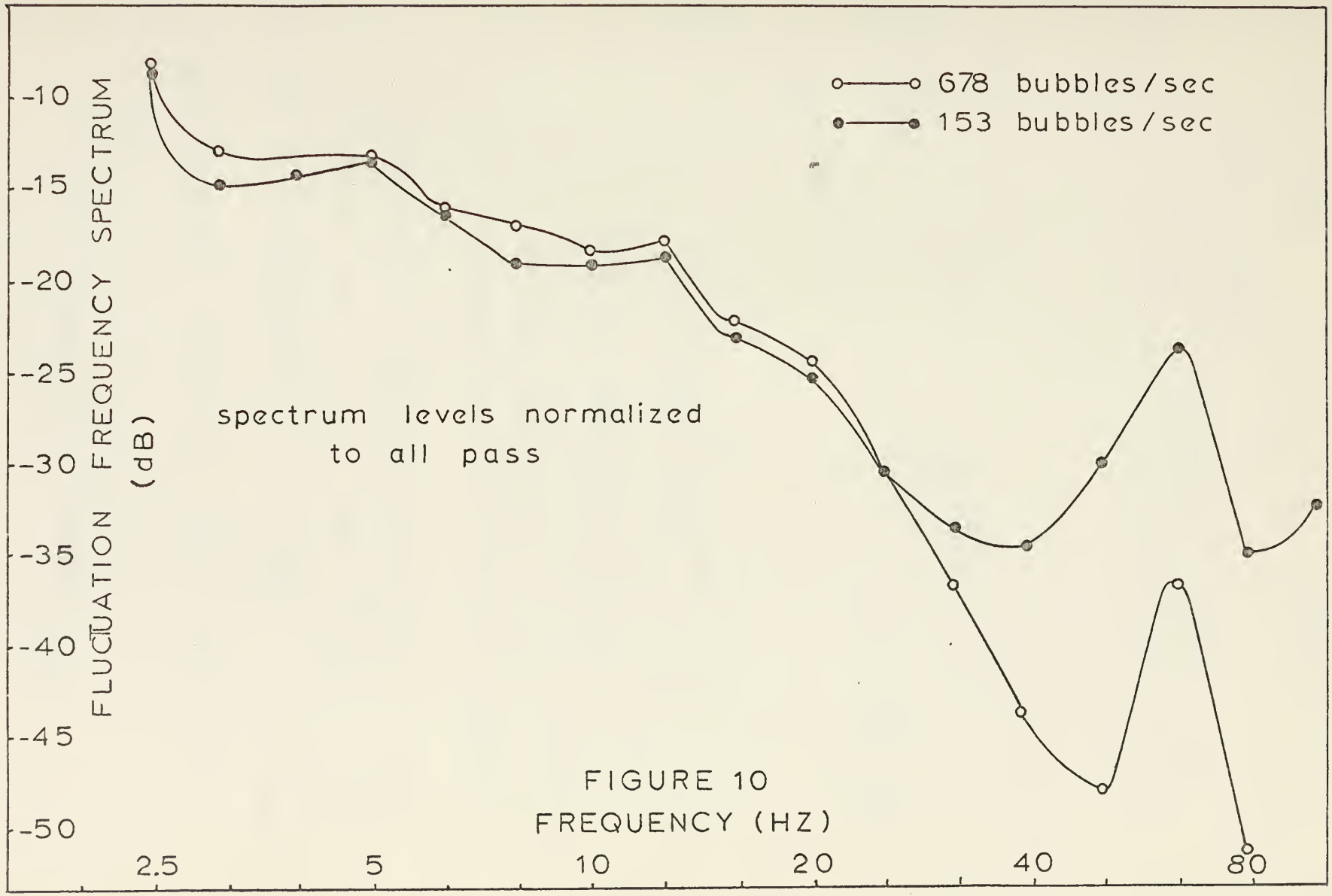
678 bubbles/sec
153 bubbles/sec
spectrum levels normalized
to all pass
FLUCTUATION FREQUENCY SPECTRUM (dB)
-10
-15
-20
-25
-30
-35
-40
-45
-50
2.5
5
10
20
40
80
FREQUENCY (HZ)

FIGURE 10

B. BACKSCATTER

1. Target Strength

The backscatter experiment was similar to the forescatter experiment except for the different geometry involved:

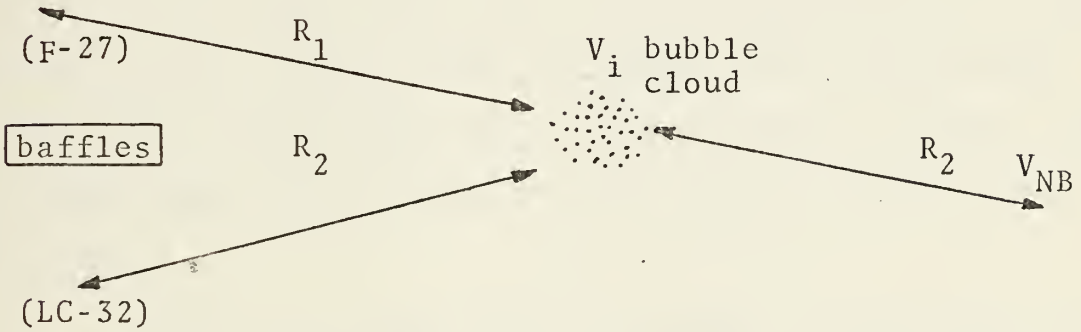

where V_i = voltage incident at the geometric center of the bubble cloud;

V_B = voltage received at LC-32 with bubbles present (backscatter voltage);

V_{NB} = voltage received at LC-32 with no bubbles present (direct path voltage);

V_r = voltage scattered by bubbles corrected to one meter.

If one assumes spherical spreading of the signals from the F-27 and from the bubble cloud, then one has the relations $V_i = \frac{R_1 + R_2}{R_1} V_{NB}$ and $V_r = \frac{R_2}{1 \text{ meter}} V_B$. From Equation 6 it follows that $TS = 20 \log V_r/V_i$, which results in the relationship

$$TS = 20 \log \frac{R_2 \cdot R_1 \cdot V_B}{(R_1 + R_2) \cdot 1 \text{ meter} \cdot V_{NB}} \quad . \qquad (9)$$

As in the forescatter case, the target strength data were obtained in the pulsed mode of operation. The received pulses fluctuated greatly, and only the peak values were recorded. The fluctuating nature of the received signal introduced uncertainty into the data, and an uncertainty of ±3dB is assigned to the data. In order to reduce the uncertainty in the data, the system was operated in the cw mode so an X-Y plot of the received signal could be obtained. The plots that were obtained were unsatisfactory, however, due to the high noise level caused by the acoustic reverberations in the tank.

Figure 11 illustrates the target strength data for the backscatter experiment. The curve is similar in shape to the forescatter curve (Figure 7), but the backscatter results are approximately 20dB lower than the forescatter results. This suggests that the bubbles may be adding incoherently for the backscatter, whereas they added coherently for the forescatter.

2. Fractional Scattering

In the forescatter section of this paper, fractional scattering per bubble was determined using Equation 8 and a coherent model for the addition of the bubbles. In this section, the definition of Equation 8 is used, but an incoherent model is used in the determination of the fractional scattering per bubble. Incoherent addition implies a different formulation:

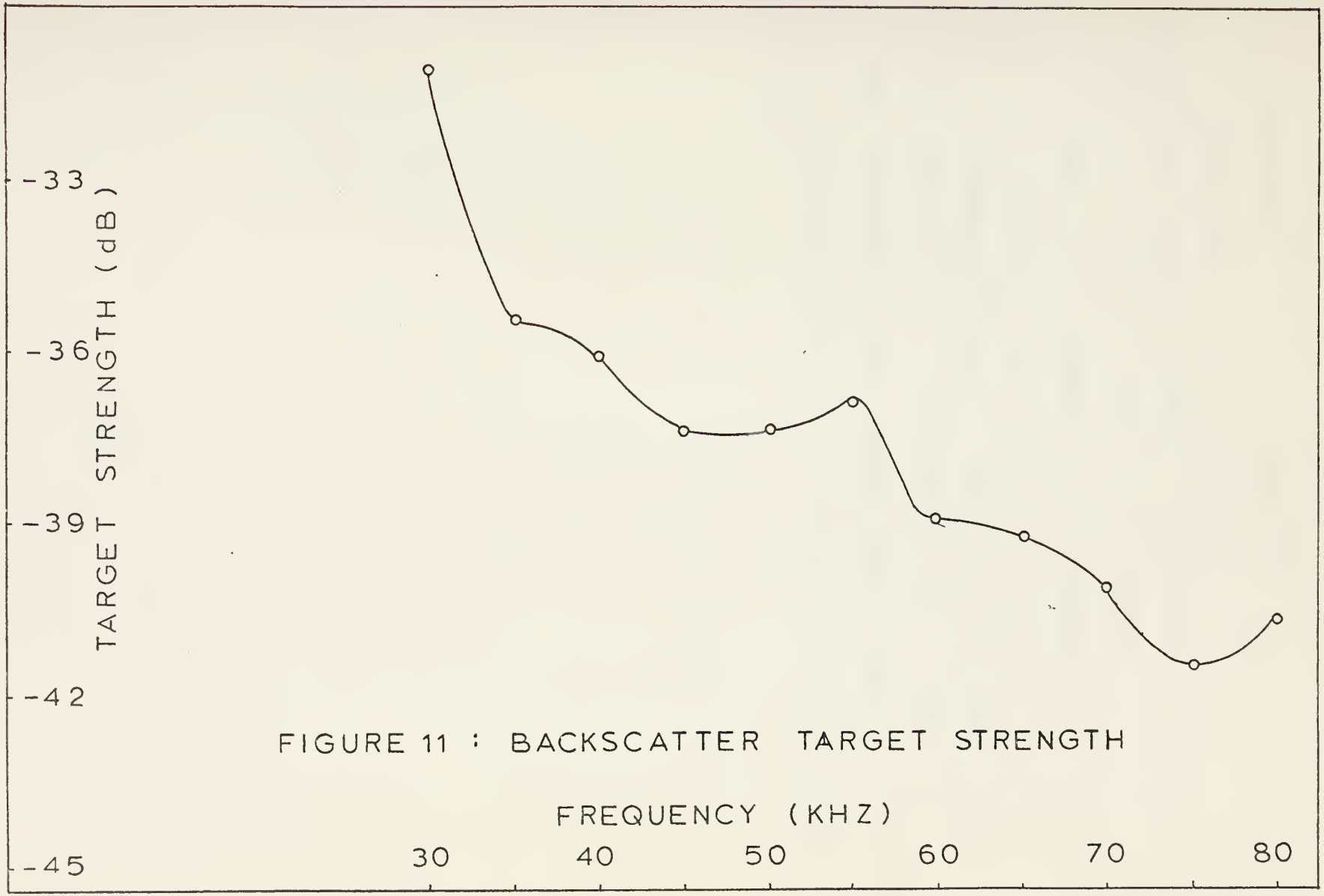

FIGURE 11 : BACKSCATTER TARGET STRENGTH

coherent: $TS = 10 \log n^2 a^2$ (10)

incoherent: $TS = 10 \log n\, a^2$ (11)

where n is the number of bubbles in the ensonified volume, and a is the fractional scattering per bubble.

Figure 12 is a graph of the fractional scattering per bubble for backscatter (assuming incoherence) and for forescatter (assuming coherence). Both curves are derived from the same bubble flow rate (296 bubbles/sec). Figure 12 strongly indicates that the assumptions of coherent scattering in the forescatter and incoherent scattering in backscatter are valid.

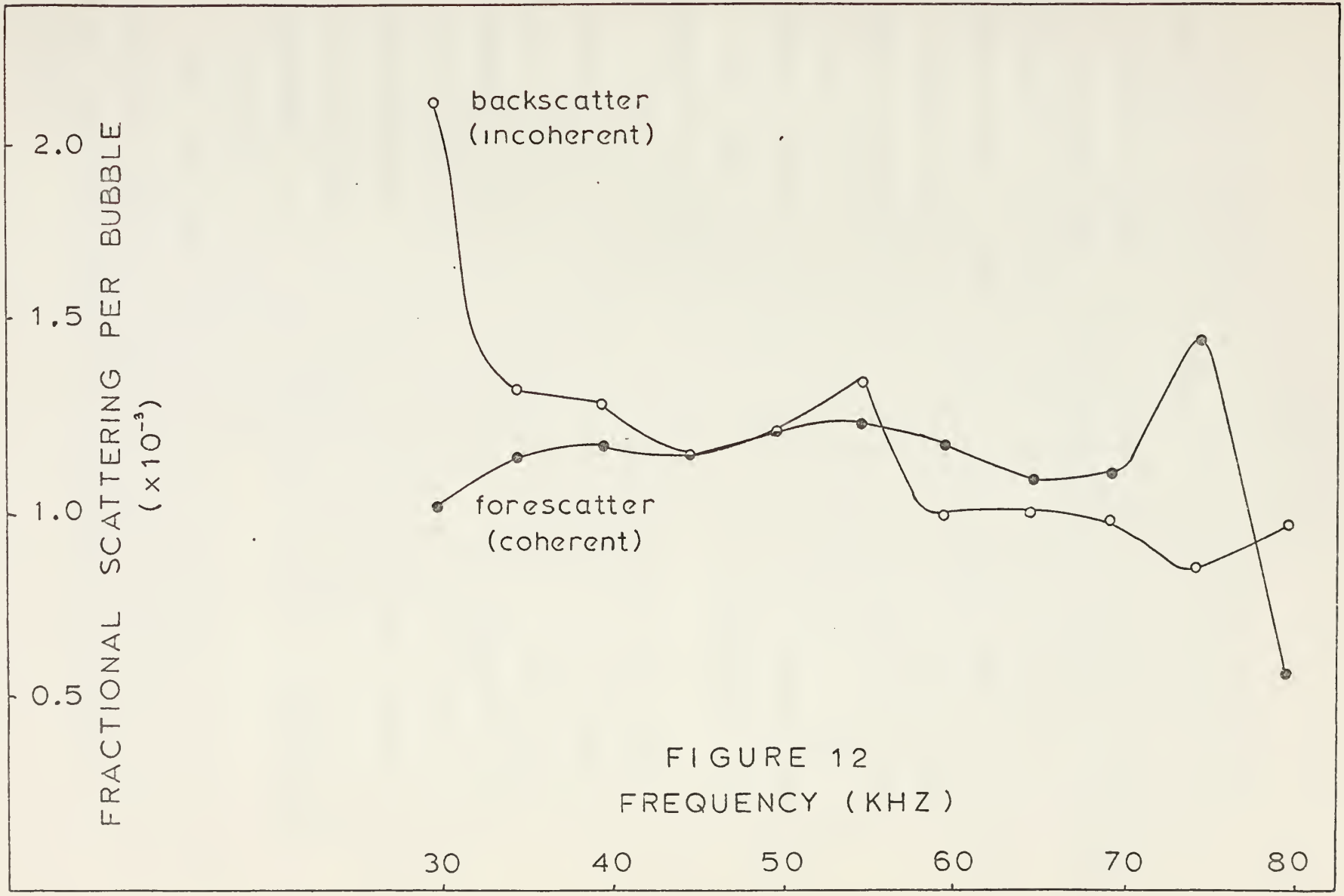
backscatter
(incoherent)
forescatter
(coherent)
FRACTIONAL SCATTERING PER BUBBLE
(×10⁻³)
2.0
1.5
1.0
0.5
30
40
50
60
70
80
FREQUENCY (KHZ)

FIGURE 12

V. CONCLUSIONS

1. In the forescatter direction, the bubbles scattered coherently. The total signal scattered by a bubble cloud is directly proportional to the number of bubbles ensonified by the sound field. In the backscatter direction, the bubbles scattered incoherently. The total signal scattered by a bubble cloud is proportional to the square root of the number of bubbles ensonified by the sound field. These results appear reasonable when one takes into consideration that the phase distribution of the radiated pressure from each bubble is that of an end-fired array in the forward direction.
2. The bubble cloud did not scatter isotropically. The preferred direction was forescatter.
3. In the forescatter, the fluctuations of the signal received at the hydrophone were between two and nine per cent of the average, tending to be higher at the lower frequencies (frequency dependent). The fluctuations were also dependent upon the bubble flow rate, increasing as the bubble flow rate increased. The fluctuation frequency spectra levels decreased with frequency, with slopes ranging from 12dB/decade in the lower frequency regions to 33dB/decade in the higher frequency regions.
4. The theoretical predictions for air requirements for the envisioned device are valid as a first order approximation. Based upon the predicted air requirements, the device is feasible.

LIST OF REFERENCES

1. Urick, Robert J., Principles of Underwater Sound for Engineers, p. 201-203, McGraw Hill, 1967.

2. David W. Taylor Model Basin Report #802, An Experimental Investigation of the Drag and Shape of Air Bubbles Rising in Various Liquids, by W. L. Haberman and R. K. Morton, , p. 18, September 1953.

INITIAL DISTRIBUTION LIST

		No. Copies
1.	Defense Documentation Center Cameron Station Alexandria, Virginia 22314	2
2.	Library, Code 0212 Naval Postgraduate School Monterey, California 93940	2
3.	Department Chairman, Code 61 Department of Physics and Chemistry Naval Postgraduate School Monterey, California 93940	1
4.	Asst Professor A. I. Eller, Code 61 Er Department of Physics and Chemistry Naval Postgraduate School Monterey, California 93940	1
5.	LT Sherman E. Wright, Jr. Route 1, Box 437-A Orange Park, Florida 32073	1

REPORT DOCUMENTATION PAGE		READ INSTRUCTIONS BEFORE COMPLETING FORM
1. REPORT NUMBER	2. GOVT ACCESSION NO.	3. RECIPIENT'S CATALOG NUMBER
4. TITLE (and Subtitle) A Proposed Tactical Antisubmarine Warfare Device Utilizing Resonant Bubbles		5. TYPE OF REPORT & PERIOD COVERED Master's Thesis; December 1973 6. PERFORMING ORG. REPORT NUMBER
7. AUTHOR(s) Sherman E. Wright, Jr.		8. CONTRACT OR GRANT NUMBER(s)
9. PERFORMING ORGANIZATION NAME AND ADDRESS Naval Postgraduate School Monterey, California 93940		10. PROGRAM ELEMENT, PROJECT, TASK AREA & WORK UNIT NUMBERS
11. CONTROLLING OFFICE NAME AND ADDRESS Naval Postgraduate School Monterey, California 93940		12. REPORT DATE December 1973 13. NUMBER OF PAGES 43
14. MONITORING AGENCY NAME & ADDRESS(if different from Controlling Office) Naval Postgraduate School Monterey, California 93940		15. SECURITY CLASS. (of this report) Unclassified 15a. DECLASSIFICATION/DOWNGRADING SCHEDULE

16. DISTRIBUTION STATEMENT (of this Report)

Approved for public release; distribution unlimited.

17. DISTRIBUTION STATEMENT (of the abstract entered in Block 20, if different from Report)

18. SUPPLEMENTARY NOTES

19. KEY WORDS (Continue on reverse side if necessary and identify by block number)

Resonant Bubbles
Target Strength
Antisubmarine Warfare

20. ABSTRACT (Continue on reverse side if necessary and identify by block number)

An experimental investigation was made of the scattering properties of a bubble cloud in a sound field in a fresh water medium. The size of the bubbles was on the order of 0.125 cm radius, and was far above resonant size for the ensonifying sound field. It was determined that the bubbles scattered coherently in the forescatter direction, and incoherently in the backscatter direction. Based upon the scattering

properties of the bubble cloud, it appears feasible to develop a device that could have tactical applications in the prosecution of long-range submarine contacts held by active sonars. Such a device would utilize the principle of resonant bubbles, and would require approximately 2.5 cubic feet of air (corrected to STP) to maintain a +20dB target strength for five minutes of continuous operation.